

Finite element simulation of meltlines

R. Akkerman, G. Rekers & J. Huétink

*University of Twente, Department of Mechanical Engineering
P.O. Box 217, 7500 AE Enschede, The Netherlands*

ABSTRACT: A study of meltlines is presented, based on finite element calculations using a Euler-Lagrange method to describe the moving free surface. For the instationary thermal and mechanical contact behaviour between polymer and mould, use is made of a penalty formulation implemented in a contact element. For the description of contact between two polymer flows (meltlines) the model has been enhanced using reptation theory describing the healing between the two fronts. Thus, a quantitative prediction can be made concerning the development of notches as well as the strength of the meltline during the filling and cooling stages of injection moulding. Finally, the results of the simulations are compared to experiments.

1 INTRODUCTION

In numerical simulations of injection moulding of polymers often the lubrication or Hele Shaw approximation is being used. This implies that effects of fountain flow, meltlines, flow around corners and sudden changes of thickness of the cavity are neglected or described poorly. However, these phenomena have a significant influence on the distribution of molecular orientation, on the internal stresses and hence the warpage of the finished product.

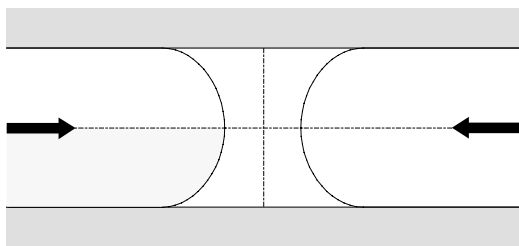


Figure 1 Two colliding flow fronts (schematically).

Meltlines are present in many injection moulded products. They may be caused by multiple gates or by splitting of the flow, e.g. by inserts in the mould. Two colliding melt fronts, as depicted in Figure 1, will weld to a certain degree. A meltline influences the optical and mechanical quality of

the product. It may be visible because of differences in brilliance, colour, distribution of fillers or because of a v-notch. In general, this is undesired.

The mechanical quality of the product is influenced by imperfect bonding over the meltline and may be worsened by stress concentrations due to a v-notch. The notch may be generated by a number of different mechanisms. Because of trapped air or increasing viscosity near the mould, the injection pressure may be insufficient to close the gap between the melt fronts. Or, the gap may have been closed, but torn open due to thermal stresses. Numerical simulation may help to reveal the origin of a v-notch.

However, experiments show notches of order 1-10 μm , in samples of order 1 mm thickness, a ratio of 1:100-1000. An accurate numerical description of an evolving notch will thus require a very fine grid and is not feasible with our current solution strategies. Zooming in on the closing notch would be a feasible alternative. The "interior boundary conditions" must be approximated in that case.

Disregarding the notch for the time being, we concentrate on the interior of the meltline. Looking on a microscopic scale (due to the fountain flow phenomenon) the macromolecules will be oriented parallel to the meltline before the melt fronts collide. By a diffusion mechanism the molecules will cross the interface after collision has taken place. Increasing the temperature or decreasing the

pressure will accelerate this process of healing, giving a higher mobility of the molecular chains.

Experimental and theoretical work can be found in literature. Implementing a model for healing in a contact element of a finite element package enables the simulation of the forming of a meltline. As a result the strength of the meltline may be predicted.

2 HEALING THEORY

Using reptation theory [de Gennes, 1971] the average interpenetration distance χ of the molecular chains over the interface can be modelled as

$$\frac{\chi}{\chi_\infty} = \left(\frac{t}{\tau_{rep}} \right)^{1/4}, \quad (t < \tau_{rep}), \quad (1)$$

where the reptation time τ_{rep} is the time needed to reach a homogeneous situation [Wool, 1981], [Bastien, 1991]. The tensile strength of the meltline, σ , is assumed to be proportional to the interpenetration depth, so

$$\sigma = \sigma_\infty \left(\frac{t}{\tau_{rep}} \right)^{1/4}, \quad (t < \tau_{rep}). \quad (2)$$

Here σ_∞ is the strength of the homogeneous material.

The parameters are influenced by the molecular weight M of the polymer. Theoretically the reptation time τ_{rep} can be shown to be proportional to M^3 , and the tensile strength σ_∞ of the homogeneous material varies linearly with $M^{1/2}$.

Apart from this, the reptation time depends on the temperature T . We use the shift factor given by the WLF equation,

$$\tau_{rep}(T) = a(T) \tau_{rep,0}, \quad (3)$$

$$\text{with } a(T) = \exp \left(\frac{-c_1 (T - T_{ref})}{c_2 + T - T_{ref}} \right).$$

Pressure dependency has been neglected at this stage. Assuming thermorheologic simplicity leads to a temperature-dependent evolution equation for the local strength of the interface

$$\dot{\sigma}(T) = \frac{1/4 \sigma_\infty^4}{a(T) \tau_{rep,0} \sigma^3}, \quad (\sigma < \sigma_\infty), \quad (4)$$

which can be integrated numerically, with temperature varying in time.

3 FINITE ELEMENTS

The polymer was modelled with a viscous/elastic material description. The material model for deviatoric deformations is simple: a (shear thinning) viscous fluid when the temperature is above T_g ,

$$\sigma^d = 2\eta \mathbf{D}^d$$

$$\text{with } \eta = \eta_0 \exp \left(\frac{-c_1 (T - T_{ref})}{c_2 + T - T_{ref}} \right) \left[1 + (s\dot{\gamma})^2 \right]^{-\frac{n-1}{2}}, \quad (5)$$

with shear rate $\dot{\gamma}$, where again a WLF-shift describes temperature dependence. Below T_g a linear elastic model is used, with a constant shear modulus G . In this stage the effects of flow induced molecular orientation on the healing behaviour have been neglected.

The isotropic part of the constitutive model is described using a Tait equation, a fit published by Zoller [1982], conveniently reproduced as

$$v(p, T) = v(0, T) \left[1 - c \ln \left(1 + \frac{p}{B(T)} \right) \right] \quad (6)$$

$$v(0, T) = v_{g,0} + A(T - T_{g,0}),$$

$$B(T) = B_0 \exp(-B_1 T),$$

where v is the specific volume and p the hydrostatic pressure and with different constants (A, B_i) above and below T_g respectively.

These material laws have been implemented in a thermomechanically coupled Euler-Lagrange finite element code, developed at the University of Twente (see e.g. [Huétink et al, 1990], [Akkerman, 1993]).

Contact was modelled using a penalty formulation: during contact the force normal to the surface is described elastically. In other words a penalty is set on overlapping surfaces; a repulsive force is generated when the *gap* between the surfaces is negative. A parallel viscous damper smoothens the open/closure behaviour. In the tangential plane the Coulomb criterion for dry friction can be used, in case of contact. The latter may be interpreted as an elastoplastic model with non-associated flow [Vreede, 1992], see Figure 2.

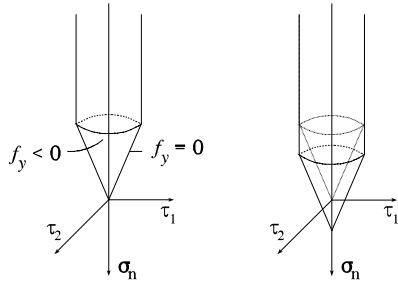


Figure 2 Slip surface in contact stress space. Right: shift of the surface due to developed strength.

The yield condition for the conical and the cylindrical part in Figure 2 can be specified as a limiting value of

$$\begin{aligned} f_y &= \tau_1^2 + \tau_2^2 - \mu^2 \sigma_n^2, & -\mu \sigma_n &\leq \tau_{max}; \\ f_y &= \tau_1^2 + \tau_2^2 - \tau_{max}^2, & -\mu \sigma_n &> \tau_{max}. \end{aligned} \quad (7)$$

When no slip occurs ($f_y < 0$), the tangential stress is proportional to the relative displacement of the two bodies in contact (linear elastic model). In case of slip ($f_y = 0$), the flow rule is most easily explained in a two-dimensional example:

$$\begin{aligned} \tau &= \mu \sigma_n, & -\mu \sigma_n &\leq \tau_{max}; \\ \tau &= \tau_{max}, & -\mu \sigma_n &> \tau_{max}. \end{aligned} \quad (8)$$

Here τ_{max} represents the radius of the cylindrical part in Figure 2. Healing is incorporated in this model by simply shifting the yield surface in the positive σ_n direction, thus admitting a tensile normal stress over the contact surface.

Thermal equilibrium for the contact element is solved by

$$\mathbf{q} \cdot \nabla - \sigma : \mathbf{D} + \sigma_e : \mathbf{D}_e = 0, \quad (9)$$

$$\text{with } \mathbf{q} = -\alpha \Delta T \mathbf{e}_n,$$

incorporating a heat transfer coefficient of the interface, α , and heat generation due to friction. The subscript 'e' denotes the elastic part of the stress and the deformation rate respectively. In the normal direction this heat balance is equivalent to

$$-\alpha \Delta T - \sigma_{xy} \Delta v_{tan} + \sigma_{xy}^e \Delta v_{tan}^e = 0, \quad (10)$$

expressed in the differences in temperature and sliding velocity on both sides of the contact element.

Finally, the healing model is implemented by integrating the strength to

$$\sigma(t + \Delta t) = \sigma(t) + \frac{1}{4} \sigma_\infty^4 \cdot \int_t^{t + \Delta t} \frac{1}{\tau_{rep}(T) \sigma^3} dt \quad (11)$$

during contact, when $T > T_g$. The accumulation of strength stops when the homogeneous tensile strength σ_∞ has been reached.

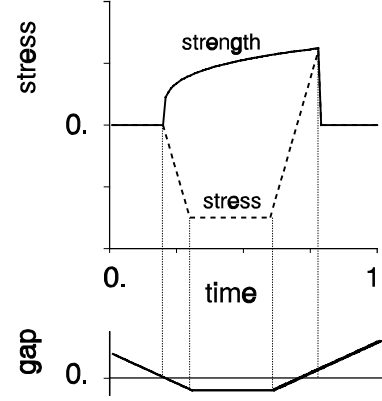


Figure 3 Contact with healing.

The behaviour of the element is illustrated in Figure 3. At a temperature above T_g a contact element is closed. When the gap is negative, the normal stress varies linearly with the gap. Strength starts building up from the moment of closure.

When the element is opened, a tensile stress can be sustained until the strength is exceeded. Strength and stress drop to zero. This discontinuous behaviour can be smoothed with the parallel viscous damper.

4 A MODEL EXPERIMENT

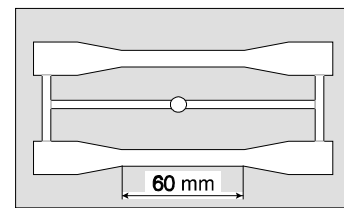


Figure 4 Experimental mould.

To check the validity of the healing model injection moulding experiments have been carried out at DSM Research. The mould in Figure 4 was filled with different materials under a number of conditions. The double gating caused a meltline in the centre of the specimen. Notches and mechanical properties were investigated by Eijpe [1990] and Carleer [1992]. One of the experimental conditions was used for a series of simulations. The pressure in the mould was recorded, and stylized as in Figure 5.

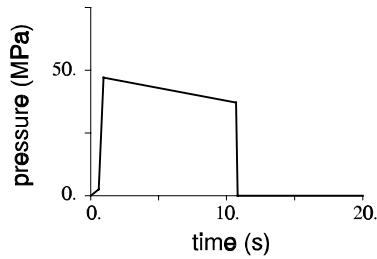


Figure 5 Course of pressure in the mould.

Further parameters are given in Table 1.

process parameters	
injection time	0.5 s
flow rate	$23.2 \cdot 10^{-6} \text{ m}^3/\text{s}$
injection temperature	503 K
mould temperature	333 K
holding time	10 s
cooling time	25 s
dimensions	
cross section specimen	3x10 mm

Table 1 Process data for healing experiment.

The material used was polystyrene (Styron 634).

5 SIMULATION RESULTS

The evolution of the meltline has been simulated by considering a cross section over the thickness of the product. A plane strain simulation was performed, eliminating effects across the width of the channel. With the given (symmetric) process conditions it is sufficient to model a quarter of the geometry (see Figure 1, dotted region).

The material data of Styron 634 are given in Table 2. For the Tait equation the data of Styron 678E were used, because the data of Styron 634 were not available. However, for a flow simulation the pvT-data are not strictly necessary so this is of minor importance. The pvT-behaviour becomes essential during the packing stage when extra material is added under high pressure to compensate for thermal shrinkage. This phase mainly determines the residual thermally induced stresses in an injection moulded product.

Previous simulations of the temperature dependent fountain flow phenomenon (Akkerman et al, 1993) showed a very limited temperature decrease in the polymer near the flow front. The thermal problem is dominated strongly by heat convection, even for this moderate flow rate. Thus,

Polystyrene (Styron 634), deviatoric		
η_0	3.1 kPa s	
s	75 1/s	
n	0.25	
c_1	14.57	
c_2	94 K	
T_{ref}	423 K	
G	1300 MPa	
PS (Styron 678E), isotropic (Flaman, 1990)		
c	.0984	
$T_{g,0}$	373 K	
$v_{g,0}$	$0.9758 \cdot 10^{-3} \text{ m}^3/\text{kg}$	
	glass	rubber
A	$.23 \cdot 10^{-6} \text{ m}^3/\text{kgK}$	$.58 \cdot 10^{-6} \text{ m}^3/\text{kgK}$
B_0	259 MPa	167 MPa
B_1	$3.0 \cdot 10^{-3} \text{ 1/K}$	$3.6 \cdot 10^{-3} \text{ 1/K}$
PS, reptation (Wales, 1976)		
σ_∞	50 MPa	
$\tau_{\text{rep},0}$	0.8 s	
c_1	20.4	
c_2	374 K	
T_{ref}	407 K	
thermal (materials and interface)		
	polymer	steel
λ	0.139 W/mK	36,35 W/mK
c_p	1.73 kJ/kgK	0,46 J/kgK
ρ	(pvT-data)	7830 kg/m ³
α	3 kW/m ² K	

Table 2 Material properties for healing simulation.

for this study we simply started with a simulation of the closing of the gap between two melt fronts. Initially, the mould was at a constant temperature of 333 K and the polymer at 503 K. In between a layer of contact elements was situated, simulating the heat transfer resistance between the two materials. During the time-stepping procedure heat was exchanged between both materials.

The frame of reference is fixed to the mould wall. The left hand side of the computational domain is kept at the same location, the lower side is stretched until the gap has closed. Only the mould behind the contact point (between mould and polymer) is taken in the computational domain. Thus, a symmetric situation is created when the gap has closed, preserving the same

element connectivity throughout the simulation.

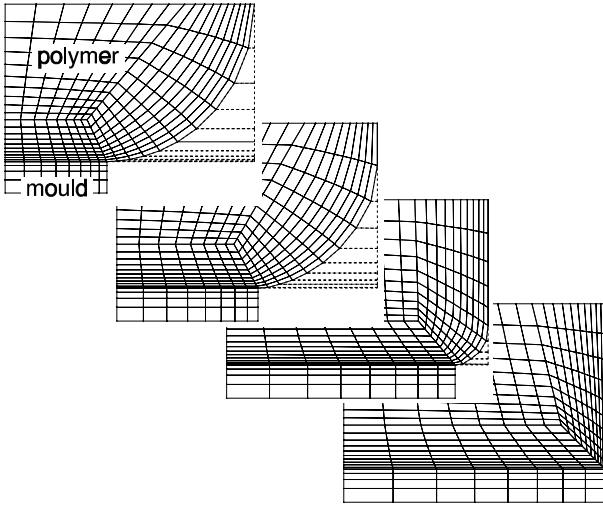


Figure 6 Closure of the gap in a number of timesteps. The dotted lines represent contact elements.

The flow of the material can be illustrated by a streamline plot.

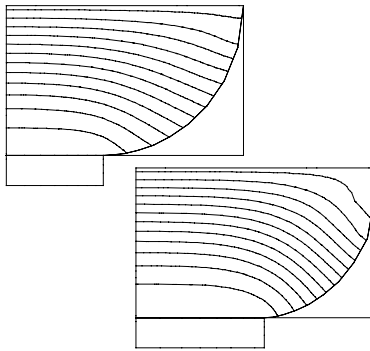


Figure 7 Streamlines during closure of the gap.

Near the meltline material is pushed towards the wall. As a result the temperature at the meltline after closing the gap is still almost equal to the entrance temperature, as depicted in Figure 8.

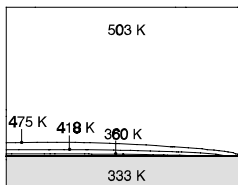


Figure 8 Temperature distribution at the moment of closure.

To simulate the development of the meltline strength, the presented mesh is still far too coarse. As the temperature near the meltline is almost independent of location, a semi 1D-model can be made to analyse the meltline strength with enough refinement to describe the details.

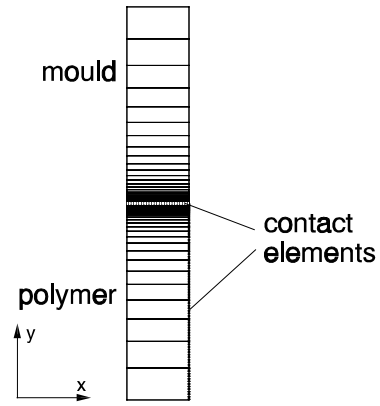


Figure 9 Element distribution for 1D simulation.

We solved the thermal problem, again starting from a cold mould (333 K) and hot polymer (503 K). In between again a contact element was placed, with a high heat transfer coefficient of $3 \text{ kW/m}^2\text{K}$ (as in Douven, 1991). The healing elements were connected to the right hand side, following the temperature history of the polymer.

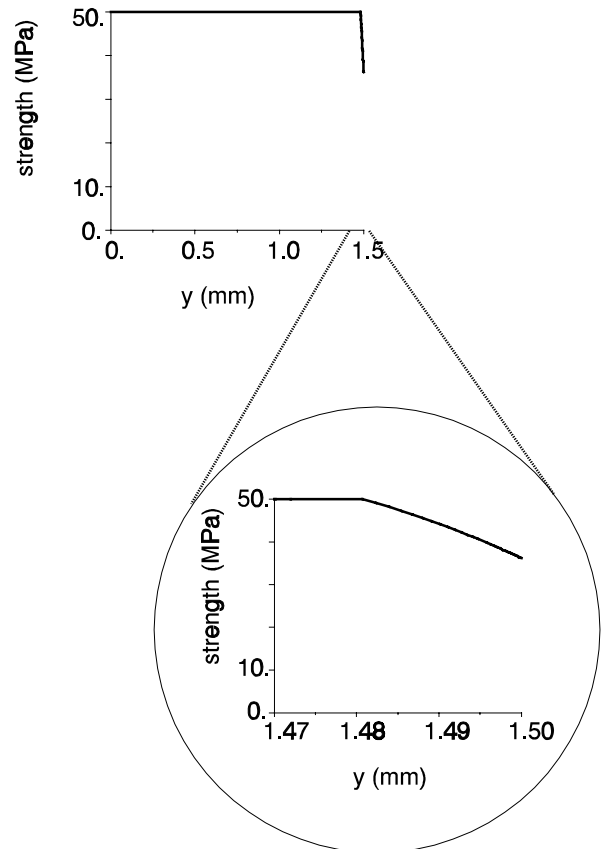


Figure 10 Final strength distribution (1D-simulation, 80 elements, gradually refined with $h_1=1000 \cdot h_{80}$).

In the core the maximum strength was reached in 0.013 s. Due to cooling a very thin layer of partial healing was found on the surface. This minimum strength converged with mesh refinement to a value of 36.3 MPa.

6 DISCUSSION

Quasistatic bending and tensile tests on the injection moulded specimens always resulted in unstable crack growth on the meltline. The process conditions under consideration lead to a tensile strength of 34 MPa. We might interpret the simulated tensile strength as a continuum stress-criterion for crack initiation. The simulated and experimental values are quite in the same range. Of course, the residual stresses will still have to be taken into account in this comparison.

Current research is directed towards accurate prediction of the internal stresses caused by injection moulding. So far, results indicate a tensile stress at the surface of a few MPa. Experimental and simulation results differ by a factor 2 at this stage, however.

The results have a great sensitivity to the value of the heat transfer coefficient between polymer and mould. For "infinite" values the strength reached at the surface drops to 6.4 MPa. For an accurate prediction reliable data have to be available. Note that the heat transfer is influenced by the surface conditions, such as roughness and contamination.

In a subsequent stage the orientation resulting from the flow simulation can be taken into account in the description of the healing process. The thermomechanically coupled problem can be solved, but research is continued to refine the results.

ACKNOWLEDGEMENTS

The support of DSM Research is gratefully acknowledged. Especially thanks to Markus Bulters and Arie Schepens for initiating the meltline research.

REFERENCES

- Akkerman, R., G. Rekers, B.D. Carleer et al 1993. Thermomechanical contact elements for healing in polymers. In M.H. Aliabadi & C.A. Brebbia (eds) *Contact Mechanics, computational techniques*, first international conference on contact mechanics 93: 103-110. Southampton: Computational Mechanics Publications.
- Akkerman, R. 1993. *Euler-Lagrange simulations of nonisothermal viscoelastic flows* (thesis). Enschede: University of Twente.
- Bastien, L.J. & J.W. Gillespie jr 1991. A non-isothermal healing model for strength and toughness of fusion bonded joints of amorphous thermoplastics. *Polymer Engineering and Science*. 31:1720-1730.
- Carleer, B.D. 1992. *Healing in finite elements, simulation of meltlines in injection moulded products* (graduate report, in Dutch). Enschede: University of Twente.
- Douven, L.F.A. 1991. *Towards the computation of properties of injection moulded products: flow and thermally induced stresses in amorphous thermoplastics* (thesis Technical University Eindhoven). Enschede: Febodruk.
- Eijpe, M.P.I.M. 1990. *Visibility of meltlines* (graduate report, in Dutch). Enschede: University of Twente.
- Ferry, J.D. 1970. *Viscoelastic properties of polymers* (2nd edition). New York: Wiley.
- Flaman, A.A.M. 1990. *Build-up and relaxation of molecular orientation in injection moulding* (thesis). Eindhoven: Technical University Eindhoven.
- Genes, P.G. de 1971. Reptation of a polymer chain in the presence of fixed obstacles. *Journal of Chemical Physics*. 55:572-579.
- Huétink, J., P.T. Vreede, & J. van der Lugt 1990. Progress in Mixed Euler-Lagrange FE simulation of forming processes. *International Journal of Numerical Methods in Engineering* 30:1441-1457.
- Vreede, P.T., M.F.M. Louwes, J. Huétink & N.A.J. Langerak 1992. Contact behaviour modelled with interface elements and tool description. In J.-L. Chenot, R.D. Wood & O.C. Zienkiewicz (eds), Numiform 92 *Proceedings of the 4th international conference on numerical methods in industrial forming processes*:565-570. Rotterdam: Balkema.
- Wales, J.L.S. 1976. *The application of flow birefringence to rheological studies of polymer melts* (thesis). Delft: Delft University Press.
- Wool, R.P. & K.M. O'Connor, 1981. A theory of crack healing in polymers. *Journal of Applied Physics*. 52:5953-5963.
- Zoller, P., 1982. A study of the pressure-volume-temperature relationships of four related amorphous polymers: polycarbonate, polyarylate, phenoxy and polysulfone. *Journal of Polymer Science*. 20:1453-1464.